Effect of Reaction Temperature on the Synthesis of TiO_2 from Titanium Slag and Sodium Hydroxide via Heat Treatment

Trung Ngon HOANG [1, 2], Tuan Anh NGUYEN [1, 2], Do Trung Kien KIEU [2, 3] *, Van Khai TRAN [2, 4], Dinh Tuan PHAN [5, 6]

[1] *Faculty of Chemical Engineering, Ho Chi Minh City University of Technology (HCMUT), 268 Ly Thuong Kiet street, Dien Hong Ward, Ho Chi Minh City, Vietnam*
[2] *Vietnam National University Ho Chi Minh City, Linh Xuan Ward, Ho Chi Minh City, Vietnam*
[3] *Faculty of Materials Technology, Ho Chi Minh City University of Technology (HCMUT), 268 Ly Thuong Kiet street, Dien Hong Ward, Ho Chi Minh City, Vietnam*
[4] *VNU-HCM Key Laboratory for Material Technologies, Ho Chi Minh City University of Technology (HCMUT), 268 Ly Thuong Kiet Street, Dien Hong Ward, Ho Chi Minh City, Vietnam*
[5] *Research Institute for Sustainable Development, Ho Chi Minh City University of Natural Resources and Environment, 236B Le Van Sy St., Tan Son Hoa Ward, Ho Chi Minh City, Vietnam*
[6] *Applied Research Institute for Natural Resources, Materials and Environment, 58/4 Tran Van Du St., Tan Binh Ward, Ho Chi Minh City, Vietnam*

http://doi.org/10.5755/j02.ms.40419

Received 6 February 2025; accepted 11 September 2025

Titanium dioxide (TiO_2) is important in many industrial fields. Industrial TiO_2 is mainly produced from ilmenite and rutile ore, two abundant global resources. Studies have shown that the calcination method with NaOH can help prepare TiO_2 from titanium slag. In this study, the effect of reaction temperature between titanium slag and sodium hydroxide (NaOH) was investigated in the process of separating TiO_2 from titanium slag. The formed product was evaluated for TiO_2 content, Fourier Transform Infrared Spectroscopy, X-ray diffraction, and Scanning Electron Microscopy to evaluate the properties. The results showed that the reaction temperature had a significant effect on the TiO_2 content of the product after separation. The TiO_2 content decreased with increasing reaction temperature. The decrease in content is due to increased hydroxyl groups in the product. At a reaction temperature of 700 °C, the product had the highest TiO_2 content of 96.78 wt.%. The results also indicated that the product's main allotropic form of TiO_2 is rutile.
Keywords: titanium dioxide, titanium slag, rutile, heat treatment, anatase.

1. INTRODUCTION

Titanium dioxide is a material with special chemical and physical properties, most notably high whiteness, chemical durability, and UV resistance. TiO_2 has three main crystal forms: anatase, rutile, and brookite, of which rutile and anatase are the most widely used [1]. TiO_2 has a very high refractive index, even exceeding that of diamond, making it an effective whitening and brightening agent in many applications. TiO_2 is widely used in the paint, plastic, paper, and cosmetics industries [2 – 4]. In particular, in paints, TiO_2 is used as a white pigment to enhance light reflectance, helping protect the surface from UV rays [5]. Additionally, TiO_2 is utilised in photocatalytic technology, where it serves as an effective catalyst in water and air treatment processes [6, 7].

There are many methods to fabricate TiO_2, the most popular of which are the sulfate and chloride methods [8, 9]. Both methods use titanium ore, such as ilmenite, as input material. The sulfate method involves dissolving the ore in sulfuric acid to produce titanium sulfate and then precipitating TiO_2 from the solution. The chloride method uses high temperature and chlorine gas to convert the ore into titanium tetrachloride ($TiCl_4$), which is then oxidized to produce TiO_2. In addition, TiO_2 fabrication methods can also include hydrothermal methods, in which TiO_2 particles are formed under high temperature and pressure conditions, or sol-gel methods, which produce ultrafine TiO_2 particles through hydrolysis and condensation processes [10, 11].

The sulfate and chloride processes are the primary industrial methods for titanium extraction, but both suffer from significant drawbacks, including the reliance on acidic digestion and high-temperature chlorination. In addition to the acid method, TiO_2 can be synthesized by alternative approaches such as the sol-gel method [12] and the hydrothermal method [13]. As an alternative, alkaline treatment at elevated temperatures has been applied as a fundamentally different route, operating under fundamental conditions. In this process, titanium compounds are first converted into insoluble sodium titanates (e.g., Na_2TiO_3), which can subsequently be separated and hydrolyzed to yield titanium hydroxide ($TiO(OH)_2$). A key advantage of the alkaline method is its ability to handle complex. Under strongly alkaline conditions, resistant mineral structures are decomposed, while common impurities such as silica (SiO_2) and alumina (Al_2O_3) are converted into soluble sodium silicates and aluminates that can be easily removed by washing. These features make the alkaline method

* Corresponding author. D.T.K. Kieu
E-mail: *kieudotrungkien@hcmut.edu.vn*

particularly promising for valorizing industrial byproducts, such as titanium slag [14].

Titanium slag is a by-product obtained from the process of producing titanium metal. TiO_2 currently does not have an effective treatment method. With a relatively high TiO_2 content, titanium slag can be used as a raw material to prepare TiO_2. Nowadays, research on the preparation of TiO_2 from titanium slag has been widely conducted, focusing on chemical and physical methods to improve efficiency and purity. The preparation process usually begins by grinding titanium slag to create a fine powder and then treating it with sulfuric acid or hydrochloric acid [15, 16]. This treatment helps dissolve impurities and release TiO_2. Some studies have shown that using catalysts and different temperature and pressure conditions can improve the efficiency of TiO_2 separation from slag [14, 17]. In addition, the pyrolysis method is also being studied to recycle titanium slag and recover TiO_2 efficiently. Recent studies have also focused on optimizing the process and minimizing environmental impacts, such as reusing chemical solutions and reducing emissions generated during production [14, 18].

Among the methods of synthesizing TiO_2 from titanium slag, calcination is the method that often gives the highest TiO_2 separation reaction efficiency. There have been many studies on the calcination method, but not many studies have investigated the influence of the reaction temperature between titanium slag and the agent on the properties of the formed TiO_2 product. In this study, titanium slag was mixed with sodium hydroxide and reacted at different temperatures. After the reaction, the product was hydrolyzed and calcined to obtain the finished TiO_2. The properties of the finished TiO_2 were investigated through X-ray fluorescence, X-ray diffraction, Fourier Transform Infrared Spectroscopy, and Scanning Electron Microscopy. The results give us conclusions about the TiO_2 product obtained at different calcination temperatures. This study contributes to improving the TiO_2 production process from titanium slag and aims for sustainable chemical industry development.

2. EXPERIMENTAL METHOD

2.1. Materials

In this study, titanium slag was the primary raw material used, an essential by-product of removing iron from ilmenite ore. The titanium slag sample was collected from the Binh Thuan province, Vietnam. The chemical composition of titanium slag is shown in Table 1 and was determined by the X-ray Fluorescence method.

Table 1. The chemical composition of titanium slag, wt.%

TiO_2	SiO_2	Na_2O	Fe_2O_3	Al_2O_3	ZrO_2	Others
92.01	2.44	1.59	1.12	1.09	0.91	0.84

In addition, supporting chemicals include NaOH and hydrochloric acid (HCl), both high-quality products from Merck, meeting stringent standards for chemical experiments. Sodium hydroxide is used in solid powder form with a purity of over 99 % to ensure the stability and accuracy of experimental reactions. Meanwhile, hydrochloric acid, a 35 % solution, optimizes efficiency and stability in chemical processing stages.

2.2. Procedure

In the study, titanium slag was treated through the following preparation steps: The initial titanium slag was washed, dried, and then ground using a planetary mill at a rotation speed of 400 rpm for 10 minutes. The particle size of the slag powder after grinding was determined by laser diffraction, resulting in an average particle size of 3.54 µm.

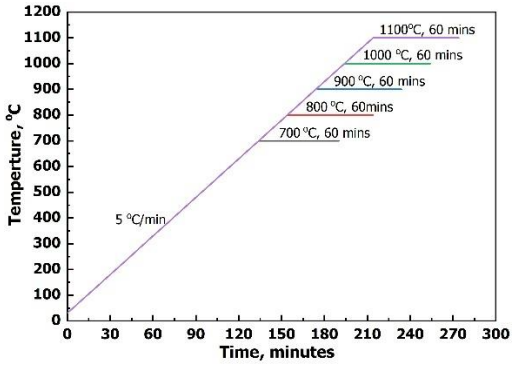

Fig. 1. Thermal conditions for calcining a mixture of titanium slag and sodium hydroxide

The ground titanium slag powder was mixed with NaOH at titanium slag/NaOH ratios of 1/1. The mixture, after mixing, was calcined in an air environment at temperatures of 700, 800, 900, 1000, and 1100 °C, with a heating rate of 5 °C/min. The dwell time at the highest temperature was 60 minutes. The heat treatment mode and sample symbols are described in Fig. 1.

After calcination, the mixture was washed with distilled water to remove excess NaOH and other soluble compounds, with a distilled water to solid phase ratio of 5:1 (volume). The washing process was carried out at 60 °C on a magnetic stirrer, heating it for 10 minutes. The solid part, after washing, continued to be hydrolyzed with 25 % HCl solution at 60 °C and distilled water at 90 °C. This process was carried out in a heated magnetic stirrer, with a stirring speed of 300 rpm for 120 minutes, to create $TiO(OH)_2$. The solid product, after hydrolysis, was dried at 120 °C and calcined at 900 °C to obtain TiO_2. The calcined TiO_2 was analyzed for chemical composition, functional group composition, phase structure, and microstructural characteristics. The goal was to evaluate the effect of the mixture ratios on the properties of the finished TiO_2.

2.3. Analytical methods

The chemical composition of the TiO_2 products was analyzed by X-ray fluorescence (XRF) to assess purity at different mixture ratios. Measurements were performed using an ARL ADVANT'X spectrometer (Thermo), with 10 g of each sample prepared in powder form. As with any analytical method, quantitative XRF is subject to potential uncertainties. In this study, the main sources of uncertainty arise from matrix effects, where fluorescence signals are influenced by variations in elemental composition, and particle size effects, related to morphological differences between powders. The reported TiO_2 wt.% values were calculated based on the total elemental titanium content,

providing a reliable basis for comparing relative purity trends across samples, which was the central objective of this analysis.

The functional group composition was determined by Fourier Transform Infrared Spectroscopy (FTIR). The equipment used was NICOLET 6700 from Thermo. The sample was analyzed in powder form, using a KBr binder, with a scan range from 480 to 4000 cm^{-1}. The scan step was set to 0.21 cm^{-1}. The FTIR results provide information on the functional group composition in the product after calcination.

The mineral phase composition of TiO_2 was determined by X-ray diffraction (XRD). The equipment used was D2 PHASER from Bruker. The diffraction angle was investigated from 15° to 75°, with a scan step of 0.02°. The sample analyzed was in powder form, helping to determine the allotropic form of the TiO_2 product. The XRD diagram was also used to calculate the crystallite size of rutile minerals through the Bragg equation [17].

$$D = \frac{0.9\lambda}{\beta cos\theta}, \quad (1)$$

where λ is the wavelength of x-ray beam (Cu K_α, with λ = 1.5418 Å); β is the full width at half maximum (FWHM in rad); θ is the Bragg's angle (in rad).

The microstructure of TiO_2 was observed by Scanning Electron Microscopy (SEM). The equipment used was JSM-IT 200 from Jeol, with a measurement voltage of 10 kV, a distance to the sample of 11.3 mm, and a magnification of 10.000 times. The SEM results provide detailed information on the form of the microstructure of the product.

3. RESULTS AND DISCUSSION

The first step in the process of recovering TiO_2 from titanium slag is to carry out the reaction between titanium slag and NaOH at high temperature. NaOH helps remove other impurity components present in titanium slag. Impurities such as SiO_2, Al_2O_3, and ZrO_2 will react with NaOH at high temperature to form soluble salts and are removed during the washing process of the product after calcination [20 – 23]. In addition, NaOH also reacts with the titanium slag component and separates TiO_2 from the slag structure. The reaction between NaOH and titanium slag at high temperature can be described through chemical Eq. 2 and Eq. 3 [24]. Na_2TiO_3 and $NaFeO_2$ are insoluble salts. In which, Na_2TiO_3 can be separated through the hydrolysis process. Thanks to that, TiO_2 can be recovered from titanium slag.

$$4FeTiO_3 + 12NaOH + O_2 \rightarrow 4Na_2TiO_3 + 6H_2O + 4NaFeO_2 \quad (2)$$

$$TiO_2 + 2NaOH \rightarrow Na_2TiO_3 + H_2O \quad (3)$$

Fig. 2 shows the evaluation results of the TiO_2 content of the samples when calcining the semi-finished product after hydrolysis at 900 °C. The results show the effectiveness of separating TiO_2 from titanium slag using NaOH calcination. The content of TiO_2 increased after separating TiO_2 from titanium slag.

The change of the sample through the synthesis steps can also be observed through the color of the sample after the stages. Initially, the slag was black (Fig. 3 a); after calcination with NaOH, the sample was green (Fig. 3 b), and finally, the calcined product after hydrolysis was white TiO_2 (Fig. 3 c).

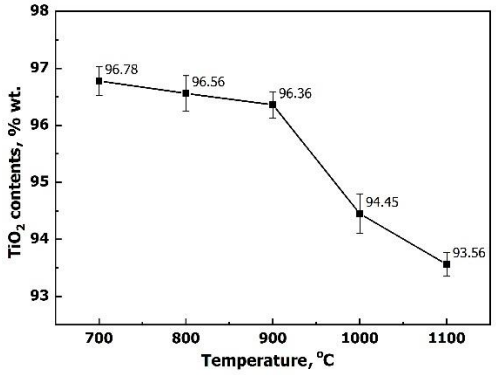

Fig. 2. The SiO_2 content of the product

The results in Fig. 2 show a clear trend: the TiO_2 content in the final product decreases as the reaction temperature between titanium slag and NaOH increases, dropping from 96.78 % at 700 °C to 93.56 % at 1100 °C. This result can be thoroughly explained by examining the physical and chemical changes throughout the synthesis process, as revealed by FTIR, XRD, and SEM analyses. If the temperature continued to increase from 900 °C to 1100 °C, the TiO_2 content in the product decreased sharply from 96.36 % to 93.56 %. Besides creating Na_2TiO_3 salt, which is beneficial for TiO_2 recovery, NaOH also reacts with other impurities in the slag. Thanks to that, impurities were removed. The rapid decrease in TiO_2 content at reaction temperatures above 900 °C also shows that 900 °C may be the limiting temperature for the reaction between NaOH and titanium slag. Suppose it is desired to increase the purity of TiO_2 in the product further. In that case, other parameters, such as increasing the heat retention time or changing the particle size composition of the initial material, can be considered.

Fig. 3. Synthesis stages of the sample: a – titanium slag; b – titanium slag after reaction with NaOH; c – calcined product after hydrolysis

The results in Fig. 2 show that the TiO_2 content in the product decreases with temperature. However, their purity is only about 93.56 % to 96.78 %. This result may be due to impurities mixed into the sample during the TiO_2 recovery process from titanium slag or some components not removed after the calcination process. To clarify this issue, the FTIR method was used to observe the functional group

composition in the samples (Fig. 4). Fourier transform infrared spectroscopy results show that the spectral form of the samples is similar. Both samples have two vibration peaks. The first peak at 483 cm^{-1} is characteristic of the vibration of the Ti-O bond [25, 26]. Ti-O is the characteristic bond of titanium dioxide. This result again proves that TiO_2 has been recovered from titanium slag by calcining slag and NaOH. The second vibration peak is at 1629 cm^{-1}. The vibration peak shows the presence of the Ti-OH bond [27, 28]. The hydroxyl group (-OH) is a chemical water bound in the structure of $TiO(OH)_2$. Many studies have shown that $TiO(OH)_2$ is a product of the hydrolysis of Na_2TiO_3 salt [29, 30].

The presence of $TiO(OH)_2$ also indicates that the calcination process to remove the hydroxyl group in $TiO(OH)_2$ has not taken place completely. The particle size of $Ti(OH)_2$ plays a significant role in the presence of residual hydroxyl groups at elevated temperatures. Higher initial reaction temperatures (700 – 1100 °C) enhance the efficiency of Na_2TiO_3 salt formation, promoting the crystallization of larger $TiO(OH)_2$ particles during the subsequent hydrolysis step.

These larger and more densely packed $TiO(OH)_2$ particles complicate the final dehydration step required to form TiO_2. As a result, samples prepared at higher reaction temperatures retain more hydroxyl groups, leading to the decrease in TiO_2 content observed in Fig. 2. Therefore, 900 °C can be regarded as the optimal temperature for this reaction; beyond this point, the adverse effects of particle growth outweigh the benefits of increased reaction efficiency between NaOH and titanium slag. This relationship between temperature and particle size is supported by XRD crystallite size calculations (see Fig. 5 and Table 2).

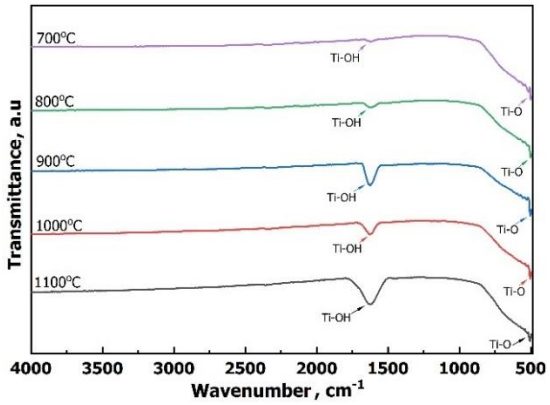

Fig. 4. FTIR analysis results of the samples

Besides FTIR, X-ray diffraction was also used to evaluate the phase composition of the product. Fig. 5 shows the XRD patterns of the samples calcined at 900 °C after hydrolysis. Similar to the analysis on the FTIR spectrum, the XRD patterns show that the main component in the product is mainly TiO_2. This once again proves that the TiO_2 content in the samples in Fig. 2 only ranges from 93.56 % to 96.78 wt.%, not entirely due to impurities in the sample but due to the existence of $TiO(OH)_2$ in the composition after calcination. The XRD analysis (Fig. 5) reveals that the sample consists of rutile (JCPDS card no. 21-1276) and anatase (JCPDS card no. 21-1272) phases.

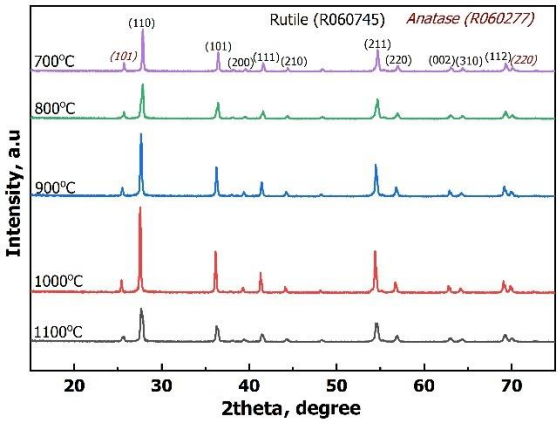

Fig. 5. The XRD patterns of the samples

Table 2. The sizes of rutile crystals, nm

Dimensions	700 °C	800 °C	900 °C	1000 °C	1100 °C
D(110)	1.81	2.76	3.19	3.89	3.97
D(101)	1.85	2.82	3.26	3.97	4.23
D(200)	1.87	2.85	3.29	4.01	5.34
D(111)	1.88	2.87	3.32	4.04	4.46
D(210)	1.9	2.89	3.35	4.07	5.24
D(211)	1.98	3.02	3.49	4.24	3.89
D(220)	2.00	3.05	3.53	4.29	4.37
D(002)	2.06	3.14	3.63	4.43	4.60
D(310)	2.06	3.17	3.66	4.46	4.83
D(112)	2.14	3.26	3.77	4.59	4.00
$\bar{D}$	1.96	2.98	3.45	4.20	4.49

Rutile is shown at the diffraction positions 27.64°, 36.28°, 39.38°, 41.43°, 44.39°, 54.48°, 56.91°, 62.92°, 64.42°, and 69.2° [31, 32]. The diffraction peaks associated with rutile are markedly more intense and sharper than the anatase ones, indicating that rutile is the predominant crystalline phase. The formation of a predominantly rutile phase is particularly significant for practical applications, as rutile exhibits the highest refractive index and superior chemical stability among TiO_2 allotropes. These characteristics render rutile the preferred material for white pigment in industries such as paints, plastics, and coatings, where high opacity and long-term durability are essential [33, 34]. Many studies have shown that the anatase allotrope will transform into rutile at ~600 °C [35]. Therefore, in the final step, $TiO(OH)_2$ was calcined to create TiO_2 at 900 °C, and the rutile allotrope was dominant. The anatase allotrope in the product is due to the incomplete allotropic transformation process.

In addition to phase identification, the XRD patterns were employed to estimate the crystallite size of the rutile phase using Eq. 1. As summarized in Table 2, the average crystallite size of the final TiO_2 product increased steadily with the initial reaction temperature, ranging from 1.96 nm at 700 °C to 4.49 nm at 1100 °C. This trend is directly related to the role of the Na_2TiO_3 intermediate. At higher reaction temperatures, Na_2TiO_3 formation becomes more efficient. During subsequent hydrolysis, the increased concentration of this precursor promotes the crystallization of $TiO(OH)_2$ by favoring crystal growth over new nucleation. Consequently, larger $TiO(OH)_2$ crystallites are obtained, which, after calcination, result in the larger TiO_2 crystallite sizes observed – consistent with the particle size

evolution revealed by SEM images. However, the rise in $TiO(OH)_2$ particle size also made the dehydration process of forming TiO_2 more difficult. This may be why the TiO_2 content in the samples with a reaction temperature of 1000 °C and 1100 °C was significantly lower than the other samples (results in Fig. 2).

In addition to phase composition, the microstructure of the samples was examined by SEM (Fig. 6) to assess particle morphology qualitatively. The SEM images corroborate the quantitative crystallite size data obtained from XRD (Table 2), demonstrating that particle size and agglomeration increased with increasing reaction temperature. These observations confirm the trend that higher temperatures promote more pronounced particle growth. The reason is that the amount of Na_2TiO_3 formed increased when the reaction temperature increased. Thanks to that, $TiO(OH)_2$ crystallizes after hydrolysis, expanding the product's particle size.

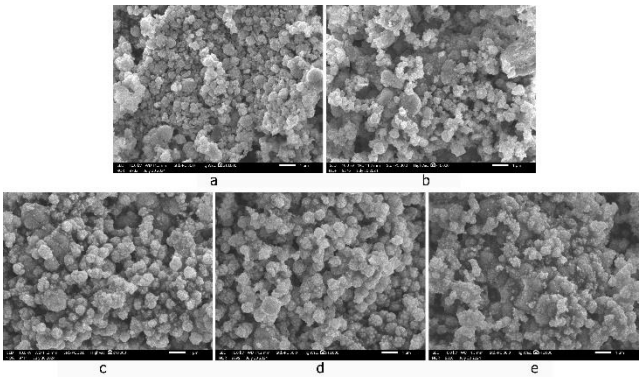

Fig. 6. The microstructure images of the samples: a – 700 °C; b – 800 °C; c – 900 °C; d – 1000 °C; e – 1100 °C

SEM analysis (Fig. 6) provided critical insights into particle morphology and its direct correlation with the final TiO_2 content. Significant morphological changes were observed as the reaction temperature increased from 700 to 1100 °C: (1) particle size increased, and (2) agglomeration intensified, evolving from discrete particles at 700 – 800 °C to large, dense blocks at 1000 – 1100 °C. This morphological evolution is directly linked to the final TiO_2 purity. The formation of large agglomerated blocks inhibits complete dehydration of the $TiO(OH)_2$ intermediate during calcination, resulting in greater retention of hydroxyl groups, as confirmed by FTIR analysis, and ultimately leading to the reduced TiO_2 content observed at higher temperatures (Fig. 2).

In addition, this phenomenon can be rationalized by considering both thermodynamic and kinetic factors. The initial reaction of titanium slag with NaOH is thermodynamically favored at elevated temperatures, facilitating the efficient formation of the Na_2TiO_3 intermediate. In contrast, the subsequent dehydration of $TiO(OH)_2$ to TiO_2 is kinetically constrained, as the diffusion of water vapor from the interior of larger or more agglomerated particles is hindered, thereby retarding the complete conversion to crystalline TiO_2. Therefore, the TiO_2 content in the product decreases at higher sintering temperatures.

4. CONCLUSIONS

This study investigated the effect of the reaction temperature between titanium slag and NaOH in the calcination method of recovering TiO_2 from titanium slag. The results show that temperature greatly affects the reaction efficiency between titanium slag and NaOH. The results of the TiO_2 content analysis show that at the reaction temperature from 700 °C to 1100 °C, the TiO_2 content in the product decreased from 96.78 % to 93.56 wt.%. The 900 °C can be considered as the limiting temperature for the reaction to separate TiO_2 from titanium slag by NaOH. The results of the FTIR, XRD, and SEM analyses show that when the reaction temperature increases, the amount of Na_2TiO_3 created promotes the crystallization process of $TiO(OH)_2$. $TiO(OH)_2$ formed with large particle size hinders the dehydration process. As a result, hydroxyl groups existed in the product samples and reduced the TiO_2 contents. XRD analysis confirmed that rutile is the predominant allotropic form of the synthesized TiO_2, representing the most thermodynamically stable phase. The dominance of rutile, characterized by its high refractive index and strong UV stability, renders the recovered product highly suitable for direct utilization as a high-performance pigment in paints, coatings, and ceramics.

Acknowledgments

We acknowledge Ho Chi Minh City University of Technology (HCMUT), VNU-HCM for supporting this study.

REFERENCES

1. **Nguyen, T.T., Edalati, K.** Brookite TiO_2 as an Active Photocatalyst for Photoconversion of Plastic Wastes to Acetic Acid and Simultaneous Hydrogen Production: Comparison with Anatase and Rutile *Chemosphere* 355 2024: p.141785. https://doi.org/10.1016/j.chemosphere.2024.141785
2. **Kamiyama, H., Nonaka, C., Saitoh, H., Ohno, M., Shimizu, Y., Isoda, K.** Anatase and Rutile Titanium Oxide Nanoparticles Induce Acute Kidney Injury by Coadministration with Paraquat, Cisplatin or 5-Aminosalicylic Acid *Die Pharmazie-An International Journal of Pharmaceutical Sciences* 79 2024: pp. 2 – 5. https://doi.org/10.1691/ph.2024.3655
3. **Topuz, B.B., Gündüz, G., Mavis, B., Çolak, Ü.** The Effect of Tin Dioxide (SnO_2) on The Anatase – Rutile Phase Transformation of Titania (TiO_2) in Mica – Titania Pigments and Their Use in Paint *Dyes and Pigments* 90 2011: pp. 123 – 128. https://doi.org/10.1016/j.dyepig.2010.12.013
4. **Pfaff, G.** Titanium Dioxide Pigments *Physical Sciences Reviews* 6 2021: pp. 679 – 696. https://doi.org/10.1515/psr-2020-0199
5. **Chaisaenrith, P., Srisawat, N., Phuangsuwan, C., Chobpattana, V., Narongchai, O., Pavasupree, S.** Development and Characterization of a Reflection Paint with Nano-Ilmenite Material for Energy-Saving in Buildings *Case Studies in Construction Materials* 20 2024: pp. e02894. https://doi.org/10.1016/j.cscm.2024.e02894
6. **Kien, K.D.T., Minh, D.Q., Minh, H.N., Nhi, N.V.U.** Study on Photocatalytic and Antibacterial Ability of TiO_2 and TiO_2-SiO_2 Coatings *Journal of Applied Science and Engineering*

28 2024: pp. 459 – 467.
https://doi.org/10.6180/jase.202503_28(3).0004

7. **Kien, K.D.T., Minh, D.Q., Minh, H.N., Nhi, N.V.U.** Synthesis of TiO_2-SiO_2 from Tetra-n-Butyl Orthotitanate and Tetraethyl Orthosilicate by The Sol-Gel Method Applied as a Coating on The Surface of Ceramics *Ceramics–Silikáty* 67 2023: pp. 58 – 63.
https://doi.org/10.13168/cs.2023.0002
8. **Zhu, K., Ren, X., Li, H., Wei, Q.** Simultaneous Extraction of Ti(IV) and Fe(III) in HCl Solution Containing Multiple Metals and The Mechanism Research *Separation and Purification Technology* 257 2021: pp. 117897.
https://doi.org/10.1016/j.seppur.2020.117897.
9. **Gordienko, P., Dostovalov, V., Pashnina, E.** Hydrofluoride Method of Complex Processing of Titanium-Containing Raw Materials *Solid State Phenomena* 265 2017: pp. 542 – 547.
https://doi.org/10.4028/www.scientific.net/SSP.265.542
10. **Tan, Z., Sato, K., Ohara, S.** Synthesis of Layered Nanostructured TiO_2 by Hydrothermal Method *Advanced Powder Technology* 26 2015: pp. 296 – 302.
https://doi.org/10.1016/j.apt.2014.10.011
11. **Vaezi, M.R., Tabriz, M.F., Kandjani, A.E., Arefian, N.A.** Effects of the pH of Initial Solution on Hydrothermally Synthesized TiO_2 Nanoparticles *International Journal of Engineering* 25 2012: pp. 131 – 136.
https://doi.org/10.5829/idosi.ije.2012.25.02b.06
12. **Chen, W.F., Mofarah, S.S., Hanaor, D.A.H., Koshy, P., Chen, H.K., Jiang, Y., Sorrell, C.C.** Enhancement of Ce/Cr Codopant Solubility and Chemical Homogeneity in TiO_2 Nanoparticles through Sol–gel versus Pechini Syntheses *Inorganic Chemistry* 57 2018: pp. 7279 – 7289.
https://doi.org/10.1021/acs.inorgchem.8b00926
13. **Zhang, X., Chen, W.F., Bahmanrokh, G., Kumar, V., Ho, N., Koshy, P., Sorrell, C.C.** Synthesis of V- and Mo-Doped/Codoped TiO_2 Powders for Photocatalytic Degradation of Methylene Blue *Nano-Structures and Nano-Objects* 24 2020: p.100557.
https://doi.org/10.1016/j.nanoso.2020.100557
14. **Chen, J., Guo, S., Omran, M., Gao, L., Zheng, H., Chen, G.** Microwave-Assisted Preparation of Nanocluster Rutile TiO_2 from Titanium Slag by NaOH-KOH Mixture Activation *Advanced Powder Technology* 33 2022: p. 103549.
https://doi.org/10.1016/j.apt.2022.103549
15. **Jing, J., Guo, Y., Chen, F., Wang, S., Yang, L.** A novel Sequential Leaching Process for Titanium Slag to Increase TiO_2 Grade to Prepare Boiling Chlorinated Charges *Hydrometallurgy* 217 2023: p.106023.
https://doi.org/10.1016/j.hydromet.2023.106023
16. **Jing, J., Guo, Y., Wang, S., Chen, F., Yang, L., Qiu, G.** Recent Progress in Electric Furnace Titanium Slag Processing and Utilization: A Review *Crystals* 12 2022: pp. 958.
https://doi.org/10.3390/cryst12070958
17. **Sui, Q.Q., Dou, Z.H., Zhang, T.A.** Phase Conversion and Removal of Impurities During Oxygen-Rich Alkali Conversion of High Titanium Slag *Transactions of Nonferrous Metals Society of China* 32 2022: pp. 1664 – 1676.
https://doi.org/10.1016/S1003-6326(22)65901-6
18. **Mālnieks, K., Mezinskis, G., Pavlovska, I., Bidermanis, L., Pludons, A.** Optical, Photocatalytical and Structural Properties of TiO_2 – SiO_2 Sol-gel Coatings on High Content SiO_2 Enamel Surface *Materials Science (Medžiagotyra)* 21 (1) 2015: pp. 100 – 104.
https://doi.org/10.5755/j01.ms.21.1.5188
19. **Djerdj, I., Tonejc, A.M.** Structural Investigations of Nanocrystalline TiO_2 Samples *Journal of Alloys and Compounds* 413 2006: pp. 159 – 174.
https://doi.org/10.1016/j.jallcom.2005.02.105
20. **Liu, Y., Zhang, Y., Dong, B., Wang, Y.** Limestone Powder Activated by Sodium Aluminate: Hydration and Microstructure *Construction and Building Materials* 368 2023: pp. 130446.
https://doi.org/10.1016/j.conbuildmat.2023.130446
21. **Thu, H.T., Dat, L.T., Tuan, V.A.** Synthesis of Mesoporous SiO_2 from Rice Husk for Removal of Organic Dyes in Aqueous Solution *Vietnam Journal of Chemistry* 57 2019: pp. 175 – 181.
https://doi.org/10.1002/vjch.201900012
22. **Widiyandari, H., Pardoyo, P., Sartika, J., Putra, O.A., Purwanto, A., Ernawati, L.** Synthesis of Mesoporous Silica Xerogel from Geothermal Sludge Using Sulfuric Acid as Gelation Agent *International Journal of Engineering* 34 2021: pp. 1569 – 1575.
https://doi.org/s10.5829/ije.2021.34.07a.02
23. **Wang, B.K., Ding, H., Zheng, Y.X., Liang, N.** Preparation and Characterisation of Amorphous Silica from Alkali Wastewater Produced in Manufacturing Process of $ZrOCl_2$ *Advanced Materials Research* 194 2021: pp. 2164 – 2168.
https://doi.org/10.4028/www.scientific.net/AMR.194-196.2164
24. **Nguyen, T.T., Pham, K.N., Dinh, T.H., Tran, V.D.N., Ullah, A.** Preparation of TiO_2 Pigment from Ilmenite Ore Concentrate by Molten Alkaline Process *Vietnam Journal of Science, Technology and Engineering* 65 2023: pp. 15 – 19.
https://doi.org/10.31276/VJSTE.65(2).15-19
25. **Chougala, L., Yatnatti, M., Linganagoudar, R., Kamble, R., Kadadevarmath, J.** A Simple Approach on Synthesis of TiO_2 Nanoparticles and Its Application in Dye Sensitized Solar Cells *Journal of Nano- and Electronic Physics* 9 2017: pp. 1 – 6.
https://doi.org/04005-1.10.21272/jnep.9(4).04005
26. **Al-Oubidy, E.A., Kadhim, F.J.** Photocatalytic Activity of Anatase Titanium Dioxide Nanostructures Prepared by Reactive Magnetron Sputtering Technique *Optical and Quantum Electronics* 51 2019: pp. 23.
https://doi.org/10.1007/s11082-018-1738-z
27. **Jin, J., Wang, X., Hu, S., Geng, J., Jing, D.** Unusual Photorheological Properties of TiO_2 Nanoparticle Suspensions under UV Light Irradiation *Journal of Physics D: Applied Physics* 52 2019: pp. 275301.
https://doi.org/10.1088/1361-6463/ab1a91
28. **Gohari, G., Mohammadi, A., Akbari, A., Panahirad, S., Dadpour, M.R., Fotopoulos, V., Kimura, S.** Titanium Dioxide Nanoparticles (TiO_2 NPs) Promote Growth and Ameliorate Salinity Stress Effects on Essential Oil Profile and Biochemical Attributes of Dracocephalum Moldavica *Scientific Reports* 10 2020: pp. 912.
https://doi.org/10.1038/s41598-020-57794-1
29. **Ngon, H.T., Tuan, P.D., Kien, K.D.T.** Effect of Titanium Slag Particle Size on The Ability to Synthesize TiO_2 by The Hydrothermal Alkaline Dissolution Method *Ceramics–Silikáty* 67 2023: pp. 328 – 333.
https://doi.org/10.13168/cs.2023.0033
30. **Ngon, H.T., Tuan, P.D., Anh, N.T., Kien, K.D.T.** Effect of The Concentration NaOH Solution on The Ability to Synthesize TiO_2 from Titanium Slag *Journal of Ceramic Processing Research* 25 2024: pp. 375 – 383.
https://doi.org/10.36410/jcpr.2024.25.3.375
31. **Tian, C.** Effects of Structural Factors of Hydrated TiO_2 on

Rutile TiO_2 Pigment Preparation via Short Sulfate Process *Scientific Reports* 10 2020: pp. 7999. https://doi.org/10.1038/s41598-020-64976-4

32. **Hipólito, E.L., Cruz, A.M.D.L.** Enhanced Photocatalytic Activity of TiO_2 Rutile by Coupling with Fly Ashes for The Removal of NO Gases *Industrial & Engineering Chemistry Research* 55 2016: pp. 11512 – 11519. https://doi.org/10.1021/acs.iecr.6b03302
33. **Morad, I., Desoky, M.M.E., Mansour, A., Wasfy, M.** Synthesis, Structural and Electrical Properties of PVA/TiO_2 Nanocomposite Films with Different TiO_2 Phases Prepared by Sol-Gel Technique *Journal of Materials Science Materials in Electronics* 27 2020: pp. 17574 – 17584. https://doi.org/10.1007/s10854-020-04313-7
34. **Saxena, R., Dwivedi, C., Dutta, V., Kaushik, S., Rakshit, D.** Nano-Enhanced PCMs for Low-Temperature Thermal Energy Storage Systems and Passive Conditioning Applications *Clean Technologies and Environmental Policy* 23 2021: pp. 1161 – 1168. https://doi.org/1168.10.1007/s10098-020-01854-7
35. **Hanaor, D.A., Sorrell, C.C.** Review of The Anatase to Rutile Phase Transformation *Journal of Materials Science* 46 2011: pp. 855 – 874. https://doi.org/10.1007/s10853-010-5113-0